THE SMALLEST OBSERVABLE ELEMENTS OF MAGNETIC FLUX

JINGXIU WANG*, HAROLD ZIRIN, and ZHONGXIAN SHI*

California Institute of Technology, Solar Astronomy, 264-33, Pasadena, CA 91125, U.S.A.

(Received 8 November, 1984; in revised form 21 May, 1985)

Abstract. We have followed disappearing elements of magnetic flux to determine the smallest elements detectable with the Big Bear videomagnetograph. All the elements followed were disappearing through interaction with elements of opposite polarity. The last remaining visible segment of magnectic field of such features can be used to infer the total magnetic flux of these and other small flux elements visible on the magnetograms.

We used both photographic and digital videomagnetograms combining 4096 Zeeman frames made at Big Bear. Fifteen elements were measured near the vanishing point, in a 2–8 hr period. The minimum observable fluxes fall in the range of 1.0×10^{16} to 1.4×10^{17} Mx, and the apparent size of these elements is in the range of 1 to 9 square arc sec. The process of disappearance appears to be a smooth one. The smallest detectable elements of network field and ephemeral regions (ER) appear to be the same as the small intra-network (IN) field elements. The present limit is still instrumental; elements smaller than 1×10^{16} would not have been detected.

1. Introduction

A number of authors (Beckers and Schröter, 1968; Stenflo, 1973; and Zwaan, 1978) have discussed the strength of elements of photospheric magnetic fields and concluded that these are concentrated in discrete bundles of fairly strong (1000 G) flux. Spruit (1977) has developed detailed models for these small structures. This general picture is supported by the fact that improved magnetograms always reveal smaller and smaller individual elements and never a uniform background field. Because the existence of these strong small fields is only indirectly established, there have been attempts to measure the smallest possible flux elements.

Simon and Zirker (1974) used spectroscopic observations to find minimum field strengths in the range 100 G to 1000 G, and sizes larger than 1.5″ in the chromospheric network. These numbers correspond to 10^{18} Mx. Because of time and field limitations they could not really search for the 'smallest flux elements". In his review of the flux characteristics of small scale magnetic field on the quiet Sun, Harvey (1977) showed examples of the intranetwork (IN) fields, and measured their flux at 5×10^{16} Mx. It is not clear if Harvey was looking for the smallest features; more likely he was referring th the typical IN fields and could have reached smaller values.

In the present work we have utilized time sequences to search for and measure the smallest possible flux elements. Because of the difficulty of deciding if a marginal small element was real, we chose shrinking elements and followed them down to the smallest detectable size. The video technique has the advantage that (1) if we observe an element

* Visiting Associates from Beijing Observatory, Academia Sinica, Beijing, China.

Solar Physics **98** (1985) 241–253. 0038–0938/85.15.

several times we know it is real and (2) if an element is shrinking we have a hope of finding it even smaller than it is now. The disadvantage of this technique is that it measures only the 'tip of the iceberg' if submergence is taking place; but it establishes the reality of measurements at this level, which may be imputed to other elements in the magnetograms. The fact of disappearance means that we really can't detect the flux if it decreases further.

The videomagnetograph at BBSO was built by Smithson and Leighton (Smithson, 1972). In 1979 it was rebuilt with a digital image processor, and in 1981 we improved the capability by installing RCA cameras with Nuvicon tubes, replacing the KDP crystal, and introducing computer programs permitting the accumulation of an almost unlimited number of frames. Introduction of a large storage disk permitted recording digital images, and the problem of calibration (using solar rotation Doppler images) has been worked out by Shi *et al.* (1985). In practice up to 4096 frames are accumulated, requiring 138 seconds of observation. The long integration time only slightly degrades resolution, because there is an enchancement effect with superposition of many elements. Under good seeing conditions, the sensitivity of the system steadily increases with number of frames, and the noise level of the 4096 frame magnetogram is arround 2 G. So although there is some distortion of strength and size, the total flux is still meaningful. The prinicpal noise sources are the vidicon, the A/D conversion, and image jitter. Sequences of such sensitive long integration videomagnetograms show that the disappearance of magnetic flux occurs frequently on the quiet Sun (Martin, 1983; Wang *et al.*, 1985). As we follow the disappearance process, we can watch flux elements shrink and determine the smallest observable flux elements.

We measured the magnetic flux of 15 of the last remaining visible segments of eight continuously shrinking magnetic features which appear continuously to cancel (by reconnection and submergence, we assume) with other magnetic features of opposite polarity during periods of 2–8 hr. Although ERs, network, and IN regions show successively weaker fields, elements of the smallest size were found in each as the magnetic knots shrank. That this is not a question of changing VMG sensitivity is attested by the appearance of constant or growing flux in other magnetic elements, and Doppler calibration of digital magnetograms a few hours apart.

2. The Identification of Smallest Visible Flux Elements

Under excellent seeing conditions on 4 September 1983, 2048 and 4096 frame videomagnetograms of the quiet Sun were obtained at Big Bear Solar Observatory. Since a number of disk areas were being studied, the interval between frames for our area was typically 30 min. The digital magnetograms are normally converted to analog form and recorded on film; at 22 : 51 UT and 00 : 27 UT two series of digital magnetograms with a range of integration times were recorded on disk and calibrated. The analog films are used to follow the disappearing elements and the two calibrated digital series, for the quantitative measurements. Thus the size of the regions is limited by their strength at the times of the two digital series. To calibrate the magnetograms we convert to Doppler

mode by introducing a circular analyzer and make a digital map of solar rotation. The method is described by Shi *et al.* (1985), and is consistent within 20%.

The photographic and digital magnetograms with 4096 frames at 00 : 27 UT are shown in Figures 1 and 2. The numbers correspond to the elements enumerated in

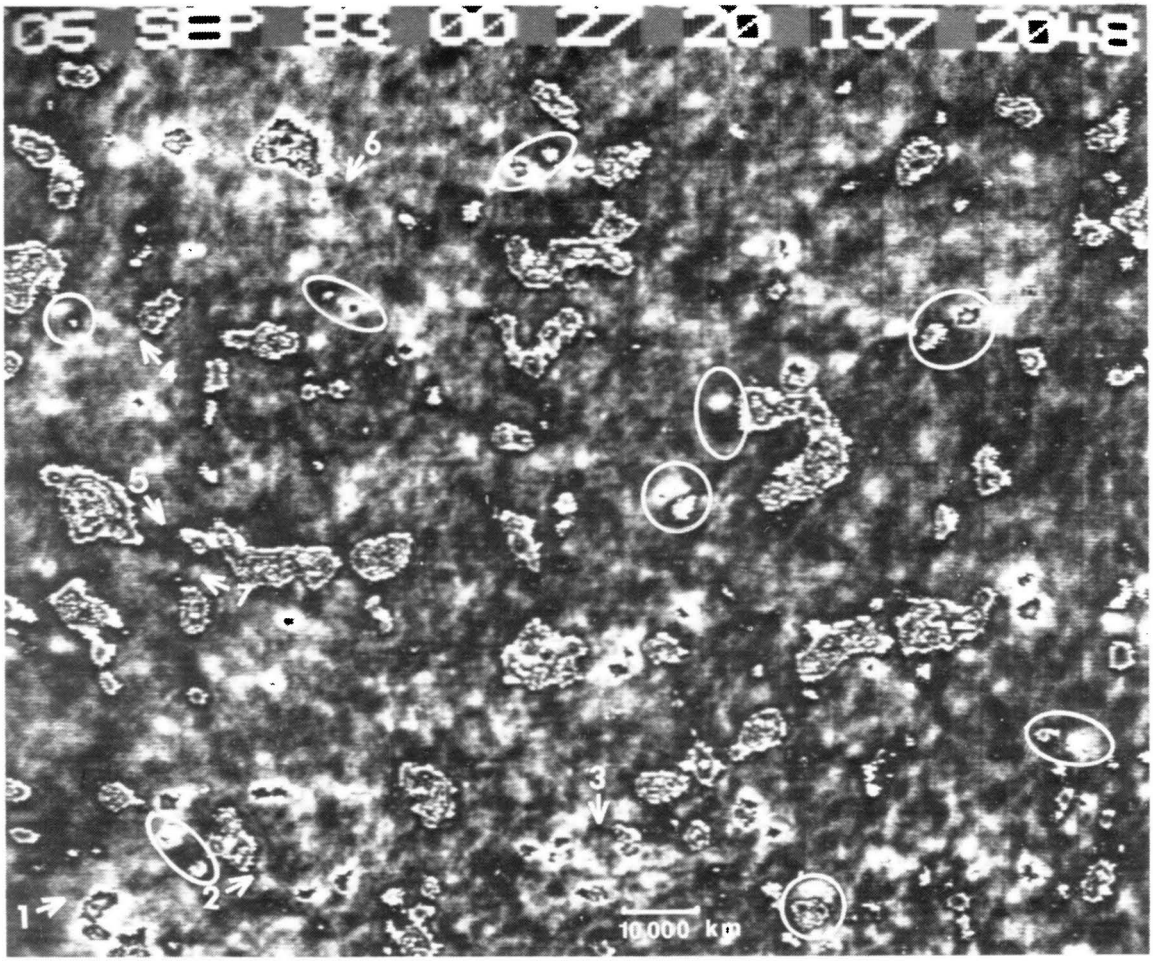

Fig. 1. BBSO 4096 frame videomagnetogram of a typical quiet region at 00 : 27 : 20 UT, September 5, 1983. The stronger magnetic features are characterized by the saturated rings which are due to a wrap-around procedure in frame addition and substraction; the resulting contours are odd multiples of the first contour. The polarity of magnetic fields are indicated by the color of the outermost part of magnetic features (white positive, black negative). The seven disappearing elements in Table I are marked by number. Nine ephemeral active regions are circled.

Table I, and illustrated in the other figures. The curious appearance of the stronger fields is due to a wrap-around procedure which reverses the output sense when strong signal fills the memory. Thus the successive brightness reversals are 1, 3, 5, etc. times the first level at which dark turns to bright or vice versa. We have compared our magnetograms with a Kitt Peak magnetogram taken earlier in the day and found them to match well. It would be possible to use disappearing elements in the analog VMG's; the result would be similar.

The data permit us to detect 9 small ERs, which are marked by circles in Figure 1.

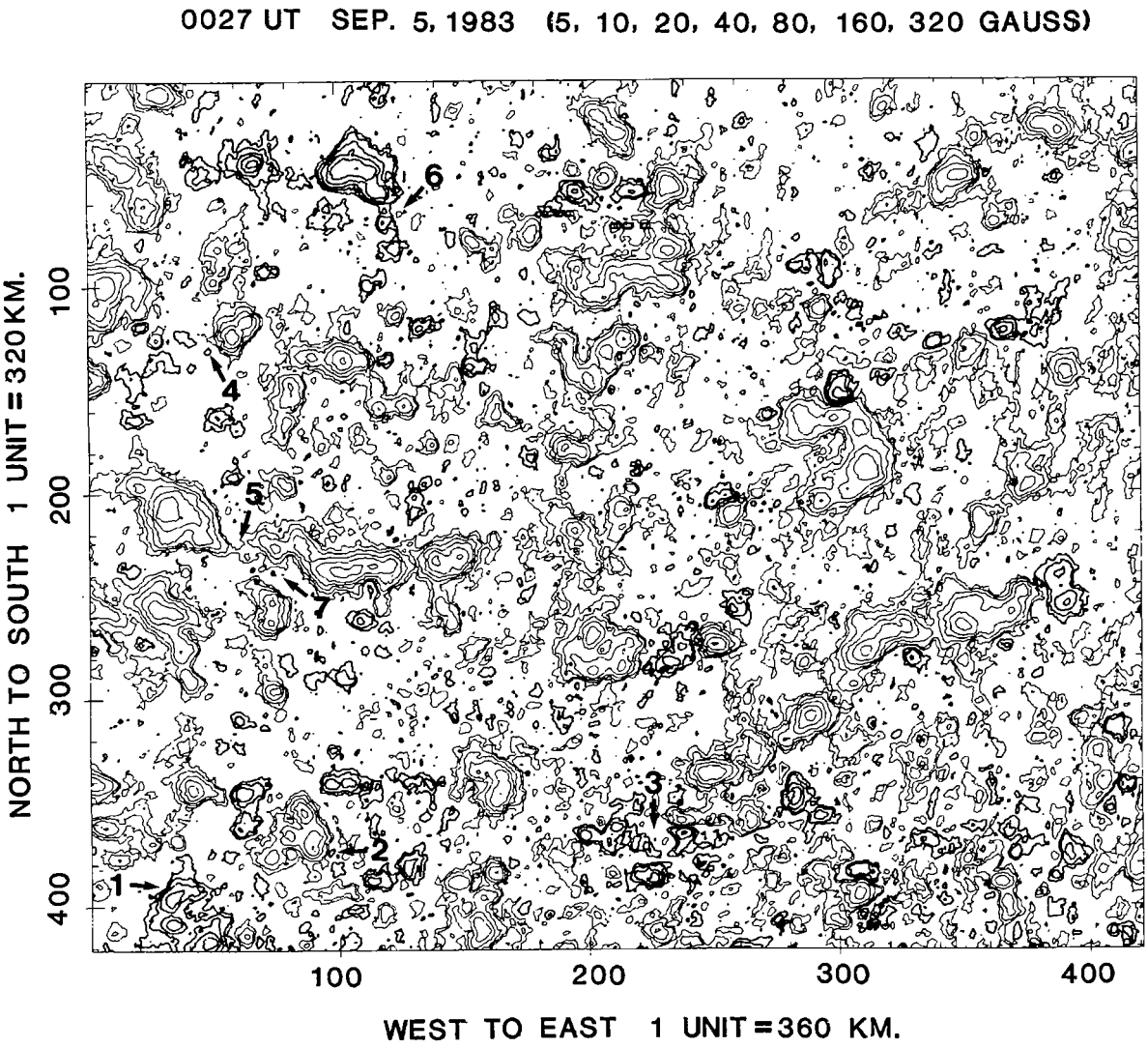

Fig. 2. Calibrated digital videomagnetogram of the same field of view and at the same time as Figure 1. The lowest contour is 5 G. The thicker line is positive polarity, the thinner line is negative polarity. The smallest visible magnetic features are indicated by the same number as in Figure 1.

We denote as ephemeral regions small dipoles more intense than the background fields which exhibit rapid growth in our sequences.

Figure 3 shows the time history of elements 1 and 2 in Figure 1. These are elements of magnetic field of sign opposite to the dominant local network which cancel with the larger network elements. Feature 1 is negative polarity near a positive polarity network feature which itself is anomalous in our field of generally negative network. In Figure 3 we see it decrease steadily* for more than 7 hr as it approaches the large network element of opposite polarity to its right; the residual feature still can be seen in the last frame. Feature 2 at the right is positive polarity and goes through the same process with an element of the dominant negative network. Since we did not see their early history we

* We only have 30 min resolution for these frames, so we cannot rule out shorter time scale jumps; but more recent data (Zirin, 1985) down to a few minutes resolution shows only gradual disappearance.

TABLE I

Examples of smallest visible magnetic features

Number	Type of feature	Class of disappearance	Time followed	Flux (10^{16} Mx)
1a	N	N–N	16 : 25–00 : 27	1.5
1b	N	N–N	16 : 25–00 : 27	1.3
2a	N	N–N	16 : 25–00 : 27	10.0
2b	N	N–N	16 : 25–00 : 27	1.7
3a	N	N–N	16 : 25–00 : 27	5.2
3b	N	N–N	16 : 25–00 : 27	2.8
3c	N	N–N	16 : 25–00 : 27	2.0
3d	N	N–N	16 : 25–00 : 27	2.4
4	N	N–N	16 : 25–00 : 27	13.6
5	E	E–N	19 : 35–22 : 51	13.0
6a	I	I–N	19 : 35–00 : 27	11.4
6b	I	I–N	19 : 35–00 : 27	1.3
7a	I	I–N	21 : 55–00 : 27	7.0
7b	I	I–N	21 : 55–00 : 27	4.8
8	unknown	unknown	19 : 35–22 : 51	4.5

don't know their origin, but they probably are the remnants of ERs. The calibrated BBSO digital magnetograms of these two examples are plotted in Figures 4 and 5, respectively. The right sides of these figures show an enlarged contour map of the smallest visible feature. The magnetic strength of each pixel has been plotted in about 0.5 arc sec intervals on the contour map. In the Figure 5 the residual feature is double on both the 22 : 51 and 00 : 27 frames, even though it is steadily decreasing.

In the last frame of Figure 3 we have enclosed within a circle a small ER which grows rapidly after 21 : 55. Its growth shows that the disappearance of the elements in Table I is not an instrumental effect.

Figure 6 shows the evolution of element 5 in Figure 1, an example of disappearance involving ERs. Three small ERs emerged rather suddenly between the 17 : 54 and 19 : 35 frames. The strongest is marked by solid line, the other two, which are not well-defined, are marked by dashed lines. The positive pole of the strongest ephemeral region steadily decreases, apparently connecting and submerging with a nearby negative fragment of network field and perhaps the other ERs. By the last frames only a tiny pole remained. The calibrated data are shown in Figure 7.

Other types of flux disappearance were also observed. The characteristics of all examples found on this day are given in Table I. We adopt the following abbreviations: N – network field, I – intra-network field, E – ephemeral region. When the element broke up into several parts, letters *a*, *b*, etc. are used. Because an element can only be definitely classed as an ER when we have seen its eruption, an 8 hr sequence prevents this identification in most cases, so only one ER disappearance is listed. The distinction between network and intranetwork is subjective; there is an apparent network of stronger, longer lived fields, and weaker, short lived elements are called intra-network.

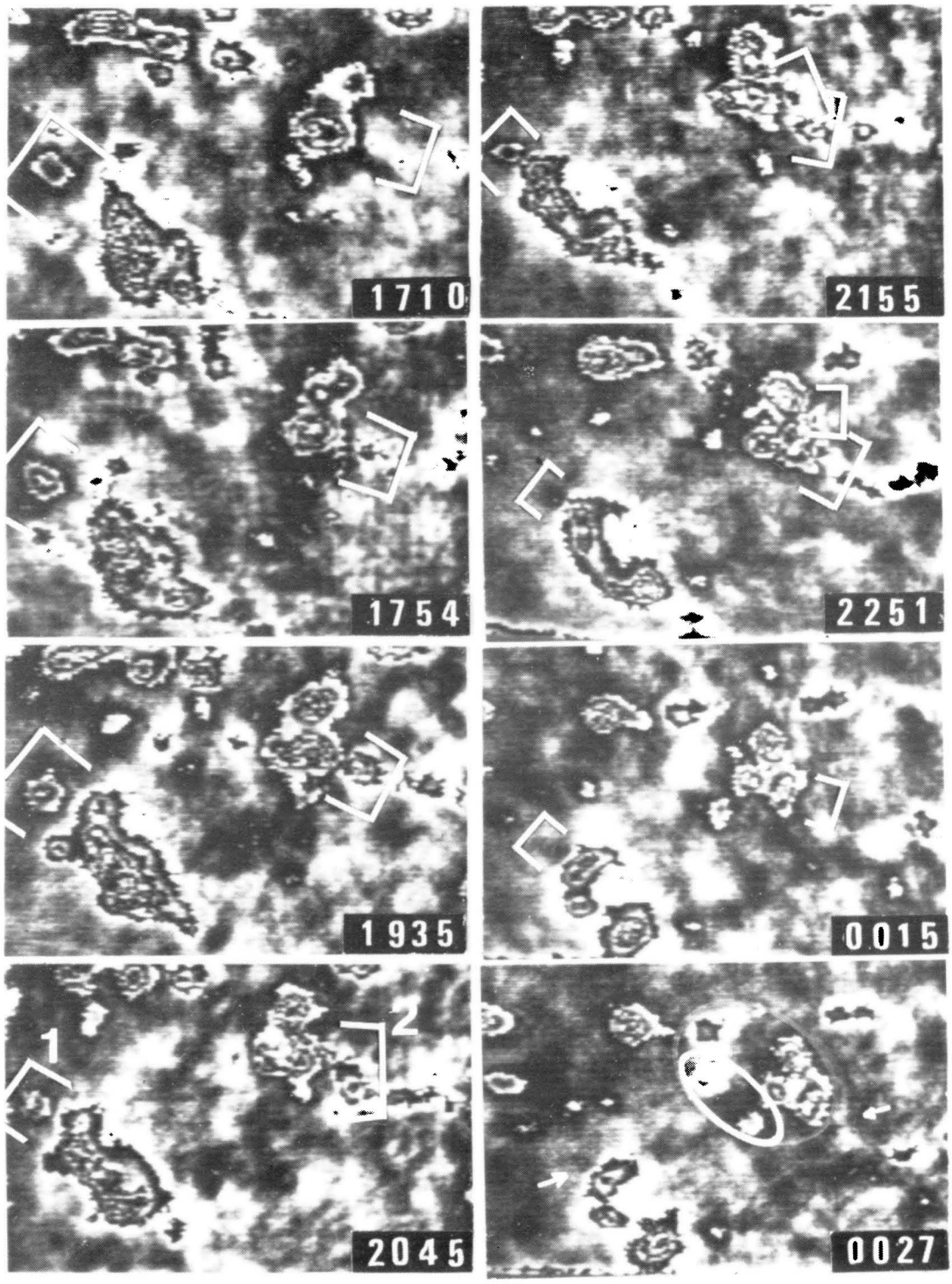

Fig. 3. The history of disappearing features 1 and 2, which are marked by open-ended rectangles and are labeled by 1 and 2. Feature 1 directly collides with a large positive network and continuously cancels with it. The mutual flux loss is revealed by losing the saturated rings and decreases in the area of both features. Feature 2 slides around a negative network and cancels with it. The smallest remaining features are marked by arrows. In contrast to the continuous decrease of flux of features 1 and 2, a small ephemeral region emerged after 21 : 55 UT and grew rapidly. It is enclosed by an ellipse on the last frame.

1985SoPh...98..241W

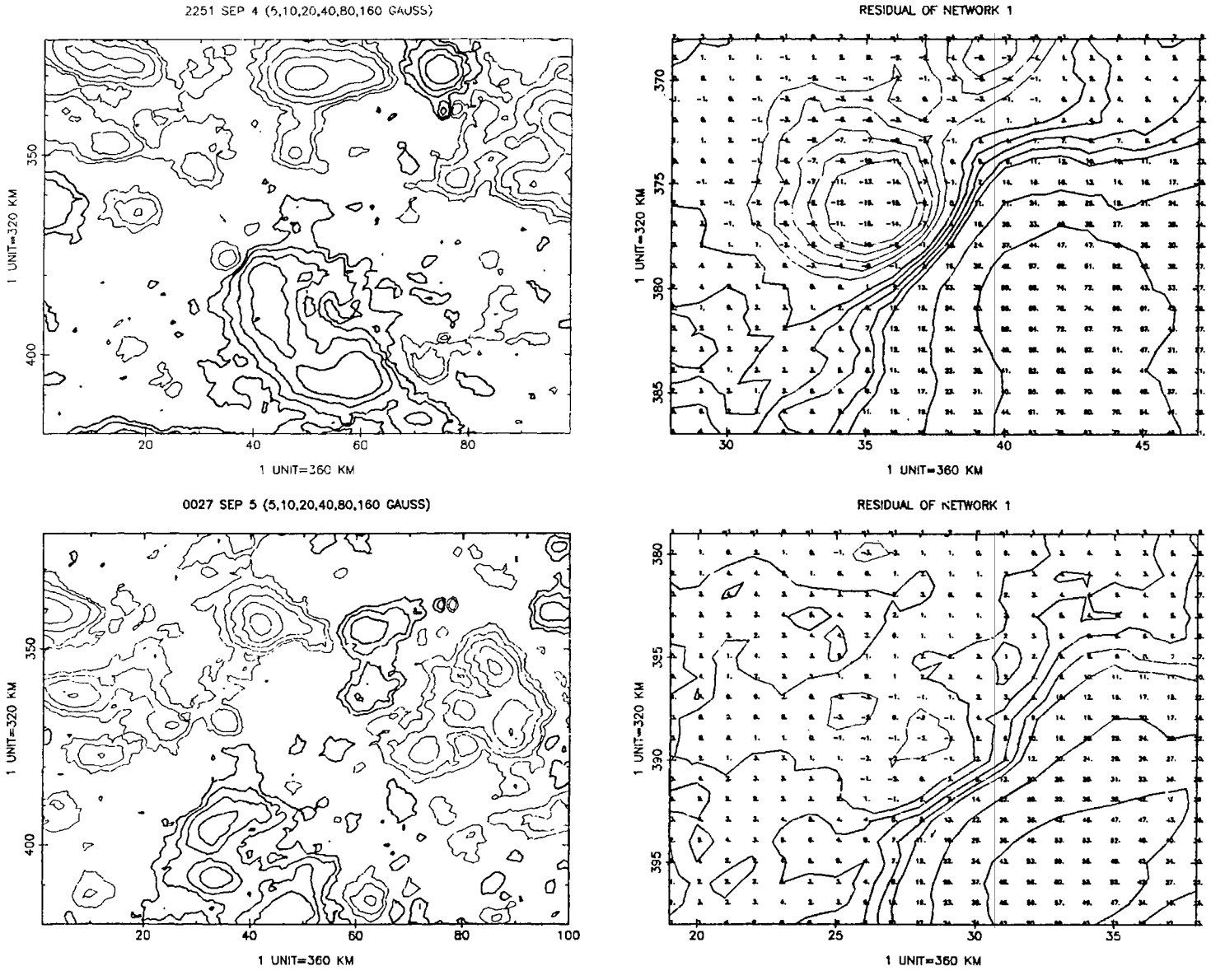

Fig. 4. Contour maps of disappearing feature 1 and its surroundings. A window around feature 1 is shown on the left side and the enlargement of it is on the right side. This reveals that the mutual disappearance of magnetic flux is a real physical process, not a seeing effect. The distance between two pixels is less than 0.5 arc sec.

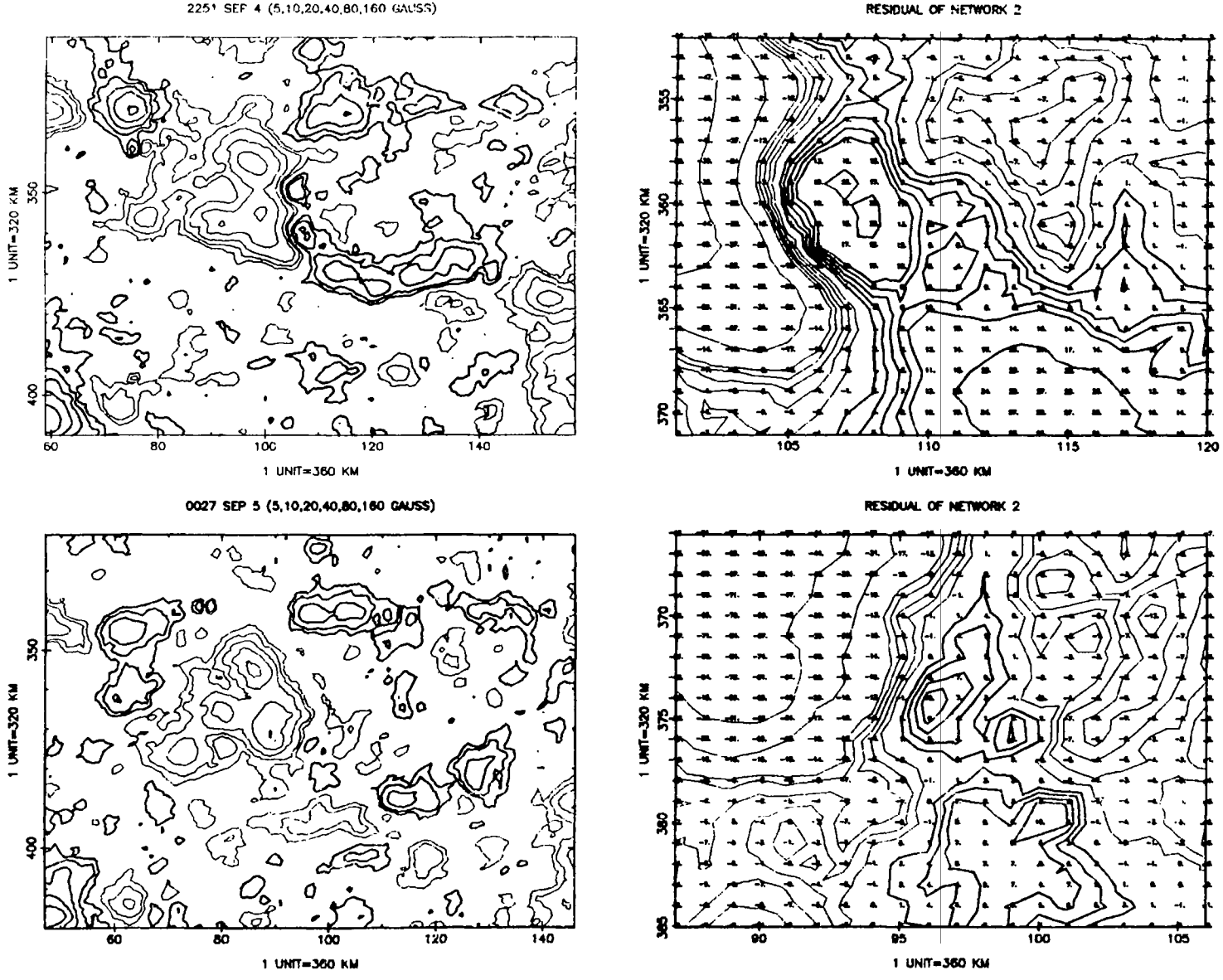

Fig. 5. Contour maps of disappearing feature 2 and its surroundings. The mutual flux loss is demonstrated by the reduction of the number of iso-gauss lines. The general pattern of feature 2 remained after the flux decrease.

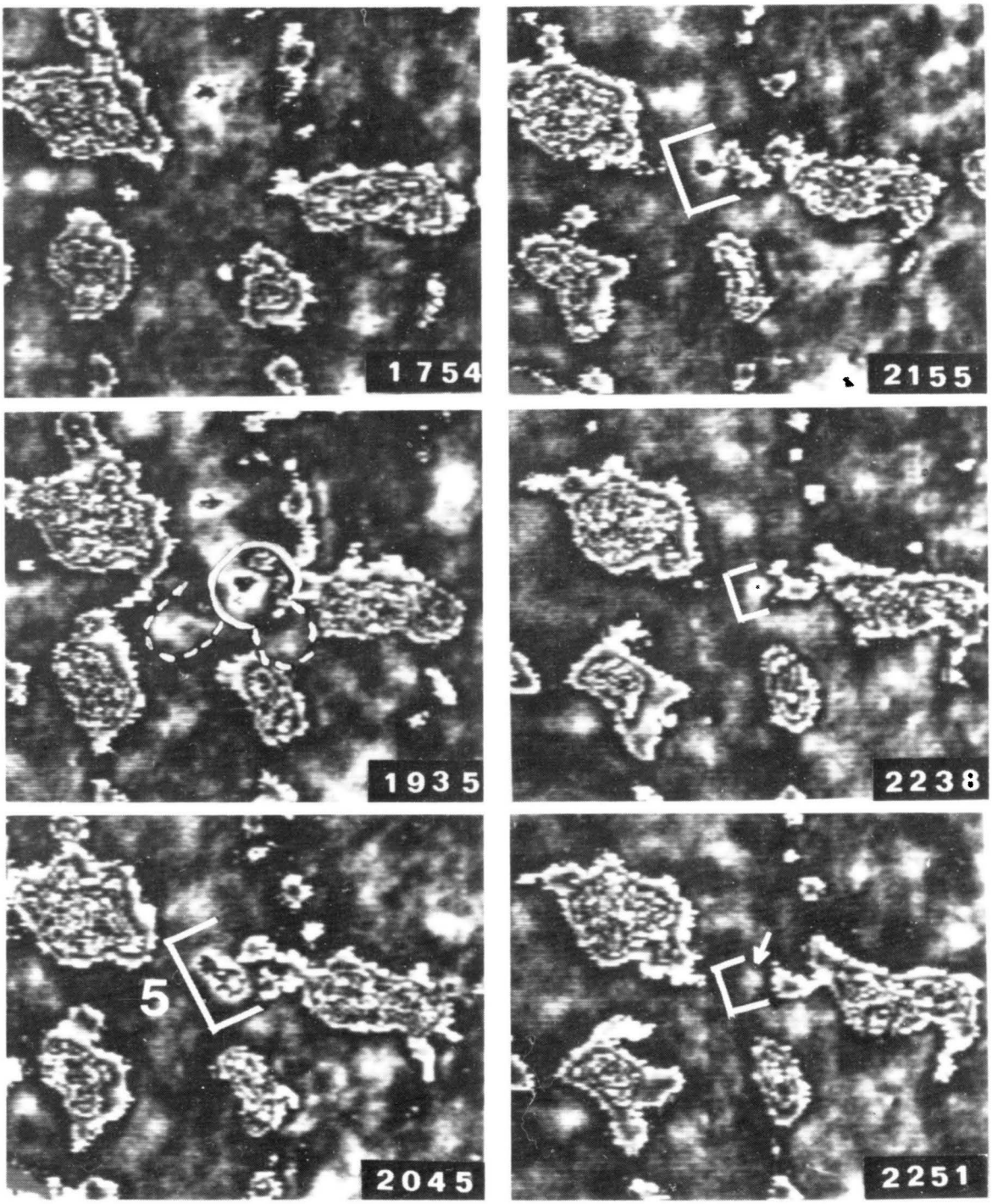

Fig. 6. The evolution of disappearing feature 5. This feature is the positive pole of an ER which emerged after 17 : 54 UT. It was continuously decreasing in size and strength while interacting with negative network or other ER features. At 00 : 27 UT this feature was reduced below the detectable limit, but its position was still marked by a numbered arrow in Figure 1.

This classification is supported by our more recent data (Zirin, 1985). In the last column we give the total flux of last and smallest visible features, using only pixels of magnetic field strength above 2.0 G. From the illustrated contours one can see that including points of weaker field will only slightly affect the total flux.

1985SoPh...98..241W

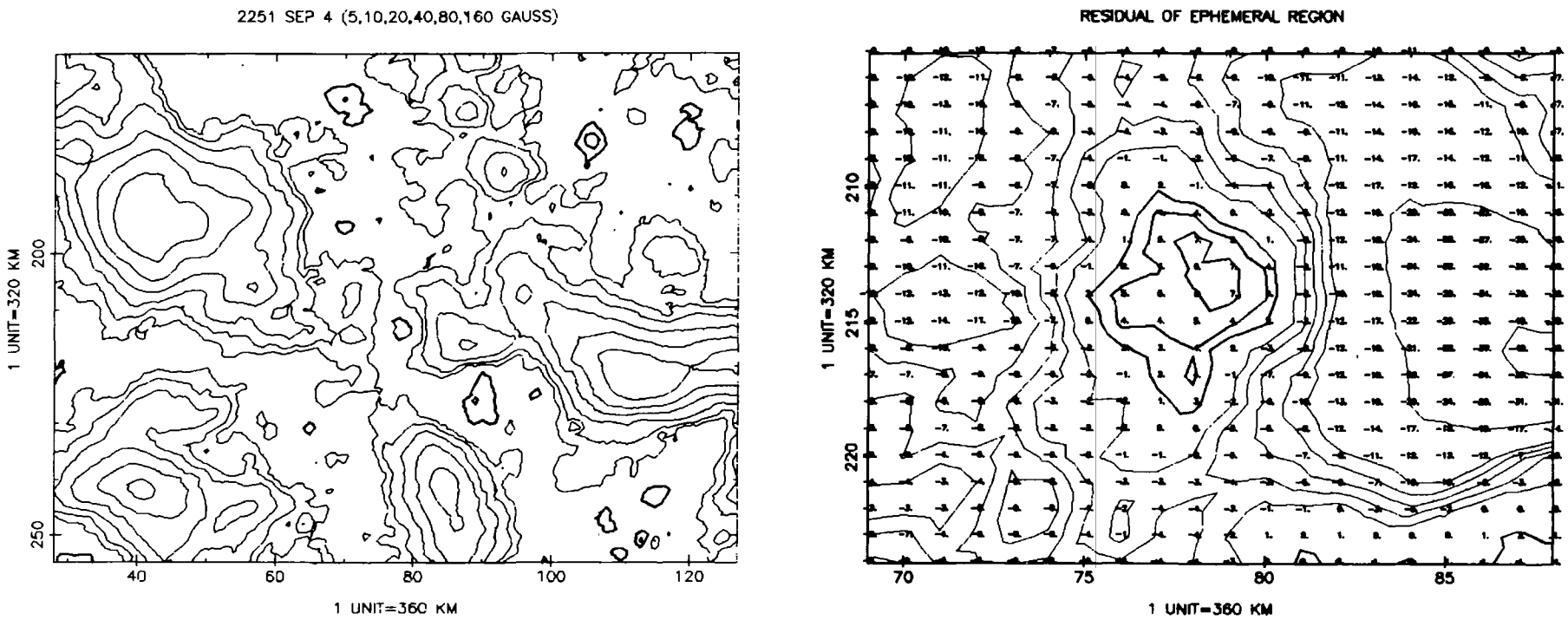

Fig. 7. The contour map of disappearing feature 5 and its surroundings at the last frame (22:51 UT) of Figure 6.

Note that it also is possible for magnetic elements to disappear by merging with like polarity, but because a stronger field element results, this process cannot be used to measure the smallest element.

We see that the smallest measured fluxes range from 1 to 14 $\times$ 10^{16} Mx, the average value being close to that mentioned by Harvey (1977). A number are in the 1–2 $\times$ 10^{16} range, somewhat smaller than previously recorded. The lower limit is set by observational constraints. The average value is set by the fact that we have but two discrete times; the analog films indicate that most features would probably have been followed down to the same lower limit if digital observations were available.

Note that the size of the smallest features is roughly the same for all three classes, so in the process of disappearance, network or ER features can be equally as small as IN features.

3. Discussion

The reality of weak features in the VMG's is normally established by their successive appearance in several frames. We have restricted ourselves to features which can be followed as they shrank for 2–8 hr, so we are certain that they are real. Most of the disappearing visible features are the residue of network elements and ERs. In any single magnetogram there are many small elements of the IN fields that are just as small, but their lifetimes are short (about an hour), and we do not have enough digital records in this run to establish their flux with certainty.

However, we have do have a series of photographic VMG's of interval 2–12 min just before the time of each digital record. Because the features appear on successive VMG's we are convinced that most of the IN features in Figure 1 and the contour map in Figure 2 are real and roughly 1–5 $\times$ 10^{16} Mx. This is in agreement with Harvey's result, although as noted he gives typical, not minimum values.

Because the magnetograph is roughly linear, the total measured flux in an element is unaffected by seeing, except for threshhold effects. The measured element size is increased by seeing, telescope jitter and pixel size (320 km, or 0.4 arc sec). Considering the all possible uncertainties and calibration errors, we estimate that the total flux values given are within a factor of 2 of the true value.

If the magnetic field strength has a magnitude of kilogauss, the real size of the smallest visible elements is about 35–130 km, and if the size is 300 km, the field strength is 15–200 G. One would expect the minimum horizontal scale to be set by the radiation mean free path; in smaller elements a temperature difference could not be maintained.

The network and ER elements are differentiated from the IN elements by lifetime and intensity. But as they disappear they shrink to the same flux as the IN elements. Therefore they must be composed of magnetic elements of roughly the same minimum size, and in fact IN elements are seen to merge into network elements. If the former represented agglomerations of some qualitatively different, much stronger elements, they could not be followed down to such small size. The fact that all are detectable to the same lower limit means that whatever irreducible stable elements of flux exist are

smaller than this level . This simply says that growing or shrinking fields that do not emerge full blown must pass through a stage when they have less flux. The fact that the last, weakest disappearing elements last up to an hour means that even these small elements are fairly stable in the hostile photospheric environment. Even the IN elements are stable for at least an hour as they move rapidly through the photosphere (Zirin, 1985).

All the elements measured here disappeared in a bipolar configuration. It is clear that a combination of reconnection and either submergence or emergence takes place to produce the loss of flux. We can reject diffusion or breakup into undetectable weak fields, because the bipolar disappearances would not be so frequent. All the flux disappearances involve magnetic elements which once were attached to something else and thus must have reconnected at some time in their history. But reconnection changes only the total magnetic energy; the total surface flux does not decrease since the same poles are present on the surface. The actual flux can only decrease by flux loops passing out of the photosphere by emergence or submergence, the separation between poles shrinking as this occurs. That is what we see. The ER elements, like feature 5 (Figure 6), emerge as part of a dipole, then disappear when they encounter a different one. We don't know when reconnection takes place, although Martin *et al.* (1985) have shown cases where small flares occurred at the flux disappearance site. In any case reconnection to the second pole must occur for flux disappearance to proceed. But flux only leaves the surface when the final loop either emerges or submerges. Can we distinguish submergence from Zwaan's (1978) suggestion that the subsurface roots have reconnected and an entire loop is leaving the Sun? The frequent occurrence of Hα fibrils connecting the disappearing elements argues against upward motion, because then we should expect the fibrils to be below the surface. Otherwise we cannot distinguish between the two possibilities.

The concept of submergence or emergence requires the disappearing dipoles to be the last visible part of a larger subsurface or horizontal element; the rest of the flux may still be present below or above the surface. But many other small elements of the same size appear on the magnetograms; the use of disappearing elements simply helps establish the identity.

4. Conclusion

The smallest observable flux elements on the quiet Sun fall in the range of one to several times 10^{16} Mx, the limit set by magnetograph sensitivity. If they contain a single intense field element, say 500 G, they must be smaller than 50 km. No difference is found between the smallest detectable elements of network, intranetwork, or ephemeral region field elements. If these features are made up of some irreducible flux elements smaller than 10^{16} Mx, there is no apparent difference between those from one feature to another. At any stage in the disappearance process one could only distinguish the different features by knowledge of their history.

Acknowledgements

We are indebted to Sara F. Martin for obtaining the observations. This work was supported by the NSF under ATM 8211002 and by NASA under NGL 05–002–034. J. Wang and Z. Shi visited Caltech through the auspices of the Academia Sinica and Caltech.

References

Beckers, J. M. and Schröter, E. H.: 1968, *Solar Phys.* **4**, 142.
Harvey, J.: 1977, *Highlights of Astronomy*, Vol. 4, Part II, p. 223.
Martin, S. F.: 1983, *Proc. of Symp. on Small Scale Dynamical Processes in Solar and Stellar Atmospheres*, Sacramento Peak Observatory.
Shi, Z. and Wang, J. and Patterson: 1985, BBSO preprint, (in preparation).
Smithson, R. C.: 1972, *Solar Phys.* **29**, 365.
Simon, G. W. and Zirker, J. B.: 1974, *Solar Phys.* **35**, 331.
Spruit, H. C.: 1977, *Solar Phys.* **55**, 3.
Stenflo, J. O.: 1975, *Solar Phys.* **32**, 41.
Wang, J., Shi, Z., Livi, S. H. B., and Martin, S. F.: 1985, to be submitted to *Solar Physics*.
Zirin, H.: 1985, BBSO preprint 0245, to appear in *Proc. of Giovanelli Memorial Symposium*.
Zwaan, C.: 1978, *Solar Phys.* **60**, 213.